

# A Design Method for High-Speed Train Nose Shape under Multi-Line Cases

Huirui Zhao<sup>1,2</sup>, Qiang Li<sup>1</sup>, Xiaofan Li<sup>3</sup>, Dietmar Rempfer<sup>3,4</sup>

**Abstract:** Different railway line cases with different object functions will result in different or completely adverse optimal nose shape. In this paper, a method for high-speed nose shape design was proposed to provide a suitable nose shape under multi-line cases. The method with emphasis on reduction of computational costs combines metamodel and numerical optimization techniques. An exemplary nose shapes under open air and passing tunnel line cases were designed by this technique. The comparison between the current CRH2 and those optimal nose shapes demonstrated the capabilities of the method.

**Keywords:** Aerodynamic, high speed train nose shape, optimization, multi-loading case, metamodel

## 1 Introduction

With the rising train speed, many engineering problems that have been reasonably neglected at low speed, are being raised, such as air drag, cross-wind effects, pressure variations inside train, pressure waves inside tunnel, impulse waves at the exit of tunnel, noise and vibration [Raghunathana, Kimb, Setoguchi (2002)] Many factors are responsible for the problems, but from the view of aerodynamics, the nose shape of the high-speed train plays a key role [Zhang (2005)]. Therefore, the study on the nose shape design and optimization is one of the most important topics in the field of high-speed train design.

---

<sup>1</sup> Laboratory for Structural Strength Testing(Beijing Jiaotong University)& China National Accreditation Service for Conformity Assessment & Engineering Research Center of Structure Reliability and Operation Measurement Technology of Rail Guided Vehicles (Beijing Jiaotong University), Beijing 100044 , China.

<sup>2</sup> Corresponding Author: Telephone:+861051688204; Fax:+861051683195; Email: shiren77@gmail.com

<sup>3</sup> Department of Applied Mathematics, Illinois Institute of Technology, Chicago IL 60616, USA.

<sup>4</sup> Department of Mechanical & Aerospace Engineering, Illinois Institute of Technology, Chicago IL 60616, USA.

Nose shape plays a key role in the aerodynamic of the train, especially with the train speed up. Thus, the design and optimization of train nose shape has aroused wide concern in the world. Ogawa and Fujii(1995) investigated the relation between the train/tunnel blockage ratio and the compression wave generated when a train passes through a tunnel, and proposed an optimal shape to reduce the micro-pressure wave [Ogawa,Fujii(1996-1997)]Iida, Matsumura,Nakatani,Fukuda and Maeda (1997) described the train nose shape with a two-parameter function, and conducted the train nose shape optimization.Kwon, Jang, Kim, and Lee.(2001); Kwon, Kim, Lee and Kim.(2001) performed a multi-objective optimization of high-speed train nose shape to reduce both the micro-pressure wave and the air drag at the same time. In 2008, Lee and Kim (2008) carried out nose shape optimization under different speeds, taking the nose shape of the G7 train as base line. Ku, Rho, Yun, Kwak, Kim, Kwon, and Lee.(2010) optimized a high-speed train nose shape for various nose lengths in order to minimize the air drag and micro-pressure wave intensity at a tunnel exit The study in Ku, Kwak, Park and Lee (2001) revealed that the optimal nose shapes differ for different nose lengths. Sun, Song and An (2010) optimized the nose shape of the CRH3 high speed train to reduce air drag, combing Kriging metamodel and MOGA-II algorithm.Vytla (2011) set up a multidisciplinary optimization (MDO) framework for high-speed train using robust Hybrid GA-PSO Algorithm. Moreover, some MDO researches on high-speed train nose shape have been carried out under the framework mentioned above [Vytla, Huangy and Pen-metsa (2010)].

Up to now, the optimization of high-speed train nose shape is limited to the one line case: passing a tunnel or in open air. Actually, the train runs under different line cases or environments, and different line case has different objectives for nose shape design. For example, an important objective for a train in open air is to reduce the air drag, while the objective in cross wind can be minimizes the lateral forces. Different objectives will result in completely different optimal nose shape. Kwon *et al.* (2001) revealed that the micro-pressure wave was weakened and the air drag was increased as the front nose shape became blunt, and therefore simultaneous reduction of the two objectives was impossible [Kwon, Kim, Lee, Kim(2001)] .

The aim of this paper is to develop a method for high-speed nose shape design and optimization under the multi-line cases. Therefore, a new design process consists of metamodel and optimization technique is proposed to provide a suitable nose shape under multi-line cases and an example of nose shape under open air and passing tunnel line cases is given.

## 2 Nose shape design technique

### 2.1 General design flow

A nose shape design can be successfully carried out via computational fluid dynamics (CFD) analysis interfaced with a formal optimization method, as shown in Fig.1 First, design variables defining the nose shape are chosen with initial values. Then the flow field around the nose shape is calculated by CFD simulation, and the object function values are obtained. Next, according to the variation information of objective function, the optimization algorithm determines whether the objective function has converged or not. If the answer is yes, the final values of the design variables define the optimum shape; otherwise, the design variables are updated, and the above process is repeated until the objective function converges to the minimum value.

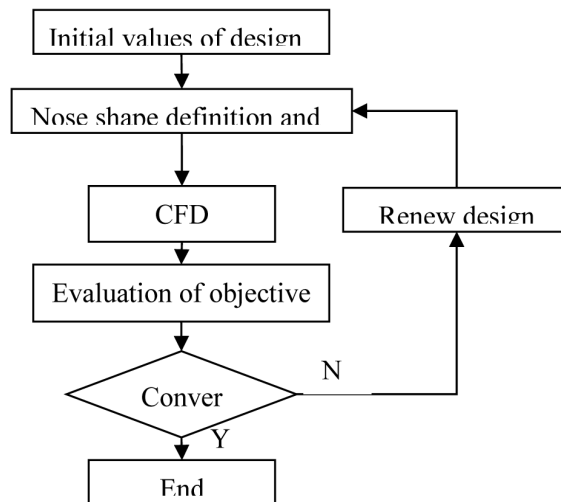


Figure 1: A generic optimization flow chart

### 2.2 Relationship among different cases

The aim of this study is to design and optimize the nose shape under multi-line cases. Therefore, we need to know the information exchange among line cases, and express it in a proper way. According to the way of information exchange between two different cases, there are three kinds of basic relationships: no information flow unilateral information flow, and bilateral information flow. The

problems corresponding to these three basic relationships are called no-coupling problem, weak-coupling problem, and strong-coupling problem, respectively. Let suppose that there are two cases: A and B, with design variables set  $X$  and response set  $Z = \{z_1, z_2\}$

### 1) No - coupling problem

If there is no information exchange between A and B during the design process, as shown in Fig.2, it is the no-coupling problem.

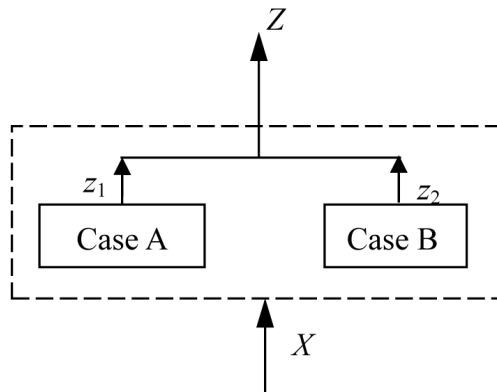


Figure 2: The no -coupling problem

The relationship between them can be described as follows:

$$f(X, Z) = \begin{pmatrix} f_A(X, z_1) \\ f_B(X, z_2) \end{pmatrix} = 0 \quad (1)$$

where  $X$  is the system design variable set,  $Z = \{z_1, z_2\}$  is response set.

As there is no correlative relationship between  $f_A$  and  $f_B$ , they can be solved separately

### 2) Weak-coupling problem

Unilateral information flow is given in Fig.3 and formula (2)

$$f(X, Z) = \begin{pmatrix} f_A(X, z_1) \\ f_B(X, z_1, z_2) \end{pmatrix} = 0 \quad (2)$$

In such a circumstance,  $f_A$  need be solved first, because its response  $z_1$  is a part of the input variables of  $f_B$

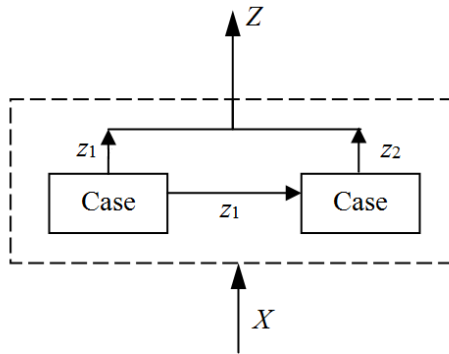


Figure 3: Weak-coupling problem

3) Strong-coupling problem

When there is bilateral information flow between A and B, the response of each case is a part of design variables of the other case, as shown in Fig.4

The relationship between them can be described as follows:

$$f(X, Z) = \begin{pmatrix} f_A(X, z_1, z_2) \\ f_B(X, z_1, z_2) \end{pmatrix} = 0 \tag{3}$$

Because both equations  $f_A$  and  $f_B$  depend on the unknown variable  $z_2$  and  $z_1$ , Eq.(3) can be solved by iterative scheme.

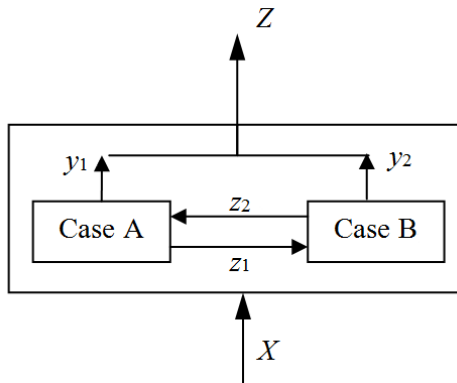


Figure 4: Strong-coupling problem

Though the relationship between two cases is very complicated in engineering, it can be categorized by one of the above three basic types, or their combination.

### 2.3 Designs of experiment and metamodel

In Fig.1, the direct interface between the analyzer and the optimization algorithm is CFD simulation, which sometimes needs lots of computational resource and often results in unreliable design solutions if the analysis problem is highly nonlinear and numerical noise is presented. Therefore, it is necessary to develop a proper metamodel (approximate model) replacing the real CFD simulation in the context of train nose shape design and optimization.

Constructing a metamodel for the computer simulations involves: (a) choosing a set of seed points  $(x_{1i}, x_{2i})$  which is considered as the sampling of the design space; (b) obtaining the set of response points  $z_{ji}$  through CFD simulation; (c) constructing a metamodel with those chosen design points  $(x_{ji}, x_{ji}z_{ji})$  as illustrated in Fig.5; (d) testing the accuracy of the metamodel. As shown in Fig.5, the region of interest is usually named as the “design space” bounded by the upper and lower limits of each of the design variables [Simpson (2001)] Choosing the location of design points for sampling the design space is a critical step to the metamodel. In order to pick representative design points, we use the method of designs of experiments (DOE).

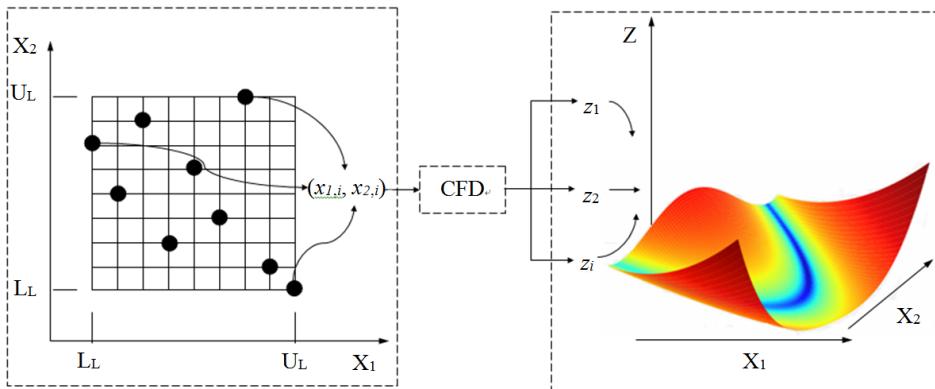


Figure 5: Progress of constructing metamodels

During optimization progress, metamodel is checked against the CFD simulation at optimal point to ensure its accuracy. If the predicted value is quite different from the CFD-based one the approximate optimization process adds additional optimal design points to the current training data set and updates the metamodel. The overall optimization procedure and its design components in the approximate optimization of the high-speed train nose shape under multi line cases, are shown in Fig.6

### 3 Nose shape design under multi-line cases

The proposed design technique is tested using nose shape design under passing tunnel and open air loading cases

#### 3.1 Line cases and objects

With the rising of train speed, the effects of aerodynamic phenomena become much stronger. One of the most serious aerodynamic problems is air drag that relates to the energy consumption of the train. As the air drag is proportional to the square of train speed, the portion of the aerodynamic drag becomes larger as the train speed increases [Joseph (2002)]. Thus, reduction of the air drag on high-speed railway train is one of the essential issues for the development of the desirable train system [Ku, Kwak, Park and Lee (2010)]

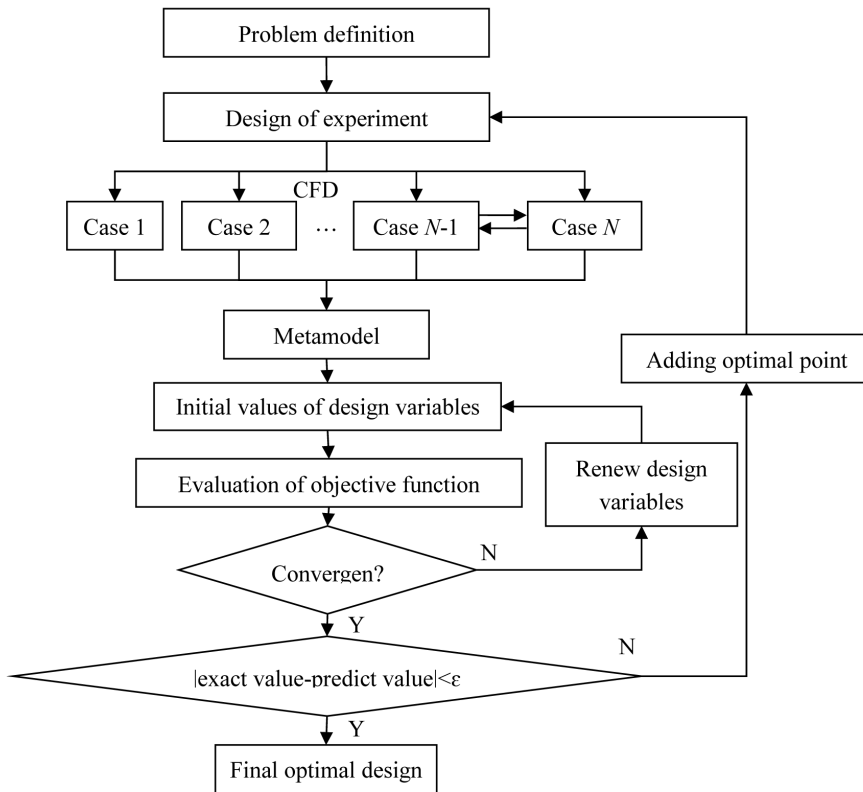


Figure 6: Overall optimization process for multi line cases

Another serious aerodynamic problem is the air pressure variation inside the tunnel when a train passes through the tunnel. The pressure variation is closely related to passenger's comfort and safe traveling of the train. As the train runs faster and faster, the pressure variation inside the tunnel has become a new type of technical problem.

These aerodynamic problems are closely related to the train shape. Therefore, nose shape design under open air and passing tunnel cases was conducted to minimize both the coefficient of air drag (CD) and the tunnel entrance pressure variation gradient (PVG). The coefficient of air drag is given by:

$$C_D = \frac{F_D}{\rho/2V_\infty^2 S_C} \quad (4)$$

where,  $F_D$  is air drag force applied to the train,  $\rho$  is the air density,  $V_\infty$  is the train speed, and  $S_C$  is the cross area of the train.

Openair case and passing tunnel case are successively joined together in most cases. To decrease the pressure gradient of the compression wave formed when a train enters a tunnel, there is usually a transition section or tunnel entrance hood installed on the ground. In this section, the air field around the train is a medium between that in open air and in tunnel. Thus, the relation between openair case and passing tunnel in this paper is considered as no-coupling.

### 3.2 Problem definition

When the compression wave is generated at the tunnel entrance, its waveform is affected by the three-dimensional shape of the train nose. However, during the wave propagation through the tunnel, the waveform changes due to energy dissipation and other non-linear effects inside the tunnel. Therefore, the compression wave can be assumed to be a one-dimensional phenomenon for the diminishing effect of the three-dimensional [Bellenoue, Morinie' re and Kageyama (2002)]. for this reason, axis- symmetric model was adopted in present project..

To get more general design space, this project added Hicks–Henne function to Iida's 2 parameters formula [Kwon, Jang, Kim, and Lee.(2001)]:

$$A(x) = \pi b^2 (1 - a_2) \left[ (1 - a_1) \frac{x}{a} + a_1 \sqrt{\frac{x}{a}} \right] + a_2 \left( \frac{x}{a} \right)^2 + \sum_{i=1}^n W_i F_i \quad (5)$$

where  $a_1$   $a_2$  are the design variables ranging from 0 to 1, to control the base line shape;  $F_i$  and  $W_i$  denote the shape function and the weighting coefficient respectively. The shape functions and the weighting coefficient ranges are given as [Kwon, Jang,

Kim, and Lee (2001)]:

$$\begin{aligned}
 F_1 &= \frac{x(1-x)}{e^{20x}}, 0 < W_1 < 0.12 \\
 F_2 &= \sin(\pi x^{0.25})^3, 0.03 < W_2 < 0.15 \\
 F_3 &= \sin(\pi x^{0.5})^3, 0.01 < W_3 < 0.11 \\
 F_4 &= \sin(\pi x^{0.8})^3, -0.05 < W_4 < 0.05 \\
 F_5 &= \sin(\pi x^{1.375})^3, -0.06 < W_5 < 0.04 \\
 F_6 &= \sin(\pi x^3)^3, -0.06 < W_6 < 0.04
 \end{aligned} \tag{6}$$

### 3.3 CFD Simulation

Axis-symmetric train models were set up separately for openair case and passing tunnel case. Predictions of CD and PVG in this paper are obtained using the numerical method RANS which is widely used in engineering. At the inlet, a velocity equal to 350km/h was used as an input boundary condition in open air simulation. In the passing tunnel case, the relative motion between the train and the tunnel is simulated by dynamic mesh. The computational domain and the boundary conditions for both cases are shown in Fig.7 and Fig.8 The convective fluxes are discredited using secondorder upwind scheme and the simulations were stopped when all the residuals have settled down below approximately  $10^6$ . All the CFD simulations in the present work were performed using the commercial software FLUENT.

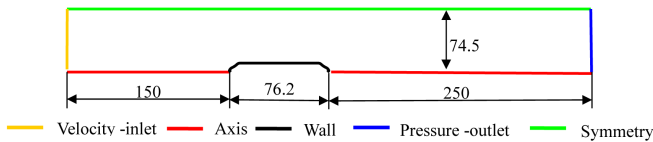


Figure 7: The computational domain and the boundary conditions for open air case

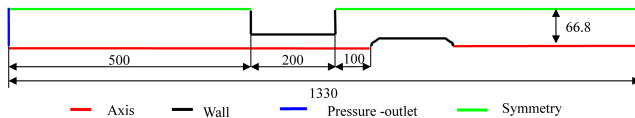


Figure 8: The computational domain and the boundary conditions for passing tunnel case

### 3.4 DOE and Metamodel

Siniša (2007) used central-composite experimental design method to generate initial seed points for response surface method (RSM), and found that the number of design points increases quickly when the number of the design variables increases. Therefore, Kwon, Kim, Lee and Kim. (2001) chose D-optimal design, which requires fewer response values than that of central-composite experimental design and is proved particularly suitable for irregularly shaped design space. Vytla (2011); Sun, Li, Zhou, Xu, Li (2011); Sun, Li, Gong, Cui, Li (2010a); Sun, Li, Gong, Cui, Li (2010) used Latin Hypercube Sampling technique to select the initial training points, because of its even distribution of samples in the given design space Lee and Kim (2001) combined Owen's random orthogonal arrays and D-optimal design to generate training data for building approximate models. That is, seed points are produced using random orthogonal arrays, while D-optimal design helps select final optimal design within seed points.

Without considering the random error and dependence on unknown parameters, it seems that D-optimal design is most suitable choice. However, uniform design (UD) was adopted in this project, for its space filling, fewer response and testing. In our case of eight design variables a total of 90 design points were obtained as Tab. 1

As for the metamodel, there are many approximation tools such as response surface model (RSM), radial basis functions (RBF), support vector machine (SVM) and so on. Among them, Kriging model is known for its remarkable performance in approximating complex engineering system. Thus Kriging model is used as a surrogate model for objective functions, PVG and CD. Kriging model has the following form

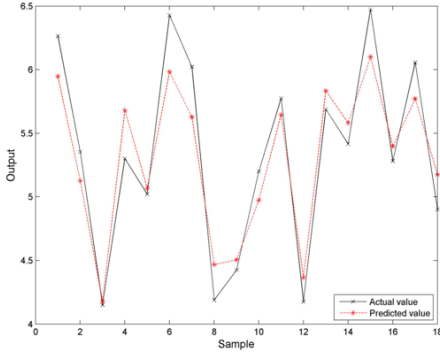
$$y(x) = f(x) + Z(x) \quad (7)$$

where  $y(x)$  is the unknown function to be approximated,  $f(x)$  is an unknown polynomial function, and  $Z(x)$  is the correlation function, which is a realization of a stochastic process with mean and variance  $\sigma^2$ , and nonzero covariance. The function  $f(x)$  in (7) is similar to a polynomial-type response surface, providing a global model of the design space.  $f(x)$  globally approximates the design space, and  $Z(x)$  creates localized deviations. More detailed description of Kriging is available in Simpson (2001)

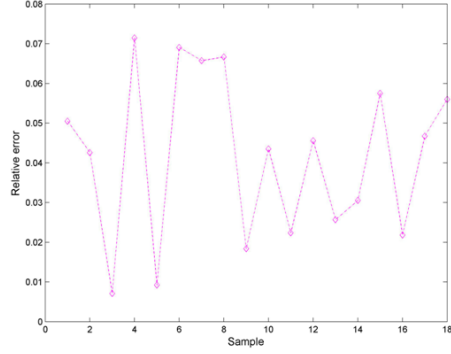
The present study applies an existing Kriging method: A second order polynomial is chosen as the basis function. A Gaussian function is employed for the correlation function, and the maximum likelihood estimation method is used to get optimal parameters of the correlation function.

Table 1: Progress of constructing metamodells

No.	$a_1$	$a_2$	$w_1$	$w_2$	$w_3$	$w_4$	$w_5$	$w_6$
1	0.0000	0.2344	0.0375	0.0769	0.0264	-0.0367	-0.0342	-0.0412
2	0.0078	0.3047	0.0497	0.0872	0.0373	-0.0211	-0.0163	-0.0506
3	0.0156	0.1641	0.0572	0.0544	0.0498	-0.018	-0.028	-0.0217
4	0.0234	0.1953	0.015	0.0741	0.0561	-0.0273	-0.0295	-0.0444
5	0.0312	0.3281	0.0037	0.0712	0.0202	-0.0461	-0.0498	-0.0373
12	0.0859	0.0938	0.0478	0.0731	0.0311	-0.0258	-0.0514	-0.0139
13	0.0938	0.3594	0.0066	0.0675	0.0405	-0.0117	-0.0553	-0.0561
14	0.1016	0.0156	0.0075	0.0684	0.017	-0.0328	-0.0225	-0.0295
...	...	...	...	...	...	...	...	...
89	0.9922	0.5312	0.0778	0.1266	0.0756	0.0297	0.0166	-0.0163
90	1.0000	0.6484	0.9863	0.1378	0.0608	0.0305	0.0173	0.015



(a) Comparison of the predicted and the actual values



(b) Relative error of predicted values

Figure 9: The accuracy of Kriging for PVG

We found that the goodness of fit obtained from training data is not sufficient to assess the accuracy of newly predicted points. Thus, 72 of 90 UD design points are selected to train the Kriging models, and the remaining 18 data points are employed to test the model’s accuracy. Fig.9 shows the accuracy of Kriging mentamodel for PVG. The max relative error of predicted value is 7.14%,which is good enough for our project.

### 3.5 Optimization Algorithms

There are several different numerical techniques that can be used to solve those global optimization problems, such as genetic algorithm (GA), particle swarm op-

timization, simulated annealing, and so on. GA has a good success rate in search and optimization problems because of its ability to use the information accumulated to exploit the initially unknown space and divide it into useful subspaces for further searching. GA are general purpose search algorithms which use principles inspired by natural evolution to find the optimum solutions to problems. The idea is to maintain a population of chromosomes, which represent a potential solution to the problem that evolves over time by controlled competition and variations. Each chromosome in the population has a fitness or ranking, which decides which chromosomes, will be used to form the new ones. The new chromosomes are formed by crossover operation. Random mutation operation based upon the mutation probability is applied to add diversity to the search process. In our study, GA toolbox in MATLAB R2009a is used to solve the optimization problem.

### 3.6 Results and Discussions

As described in the previous section, a Kriging model was obtained. A GA-based approximate optimization was sequentially conducted until the absolute difference between the approximate optimal solution and actual CFD data is within 1.0%.

There are two objectives in this project minimizing both  $C_d$  and PVG. A typical function for optimization problems with two objective functions is given by

$$f = \frac{\alpha f_1 + \beta f_2}{\alpha + \beta} \quad (8)$$

where  $f_i$  ( $i=1, 2$ ) are objective functions,  $\alpha$  and  $\beta$  are the corresponding weight coefficients.

The selection of  $\alpha$  and  $\beta$ , which have a significant effect on the final optimum shape, should take account of railway practical reality. Optimization was performed using different weights:  $\alpha$  ranging from 20% to 100%. Fig.10 shows the optimization process with  $\alpha=100\%$ , which implies that the objective of the optimization is to reduce the PVG only. Figure 10(a) shows the reduction process of PVG, while history of the predicted value of CD is shown in Fig.10 (b). It is obvious that the CD increased during most of the optimization process, that is, these two objective functions contradict each other.

The optimum shape parameters for different weights  $\alpha$  and  $\beta$  are shown in Tab.2. From Tab.2 it is evident that there is a slight drop in CD when the weight  $\beta$  increases, but at the same time PVG decreases. The result agrees with our observation shown in Fig.10. Using the data presented in Tab.2, we plot the optimum nose shapes in Fig.11

Attention was given to the optimum nose shapes,  $\beta$  varying from 0% to 80%. With the increase in the weight  $\beta$  the slope of cross section area decrease, that is, the cross

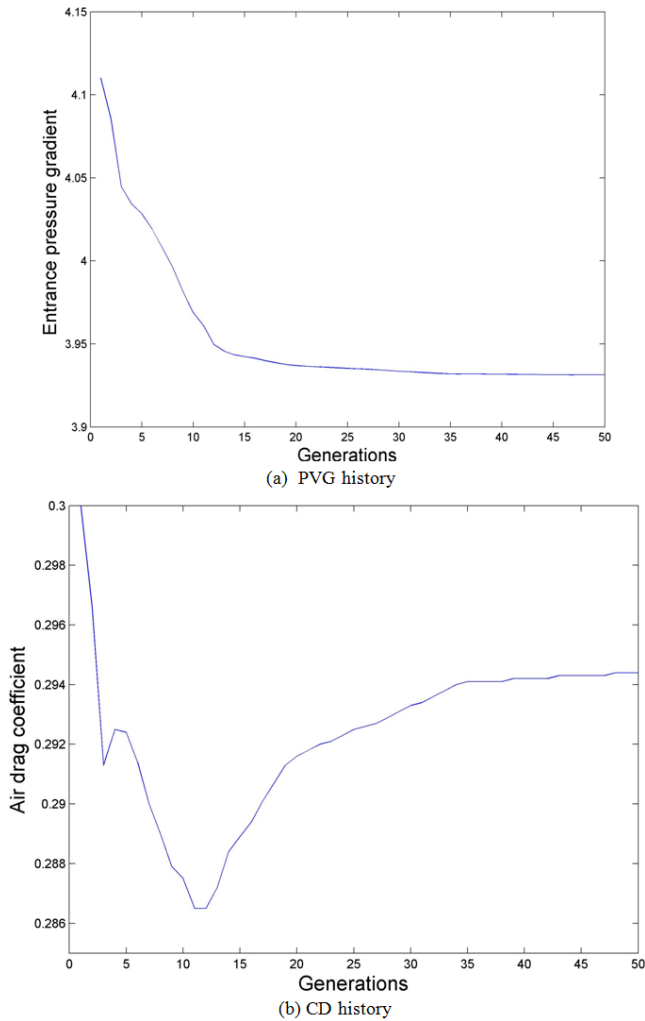


Figure 10: Optimization progress with  $\beta = 0.0\%$

section area of increases gradually to the rear, which is good for drag reduced. On the other hand, the optimal nose is blunter when the objective is to reduce PVG corresponding to small  $\beta$

Next, we compare the values of CD and PVG of the optimal shapes in Fig.11 with that of the current China high-speed train, as shown in Tab.3. Compared with those of CRH2, aerodynamic characteristics of those optimal nose shapes are improved to varying degrees. We note that the model of CRH2 was modified so that it can be

Table 2: : Uniform Design

No.	X								$f_1$ (PVG)		$f_2$ (CD)	
									$\alpha$	Value	$\beta$	Value
1	0.6568	0.00	0.12	0.03	0.01	0.05	-0.06	0.041	1.00	3.931	0.00	0.3088
2	0.00	0.00	0.12	0.03	0.01	0.05	-0.060	-0.06	0.80	3.987	0.20	0.2499
3	0.00	0.00	0.12	0.03	0.01	0.05	0.040	-0.06	0.50	4.148	0.50	0.2476
4	0.00	0.295	0.12	0.03	0.01	0.05	-0.016	-0.06	0.20	5878	0.80	0.2479

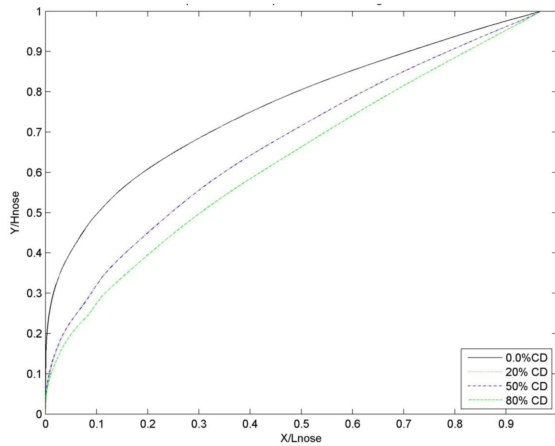


Figure 11: Optimum nose shapes with different weight values

compared with the optimal shapes obtained in the study Fig.12 shows the original and the modified nose shapes of CRH2.

Table 3: : Optimization progress with  $\beta=0.0\%$

No.	$f_1$ (PVG)			$f_2$ (CD)		
	$a$	Value	Reduction	$\beta$	Value	Reduction (%)
Base		6.4503	0		0.31586	0
1	1.00	3.862	40.12%	0.00	0.3088	0.62%
2	0.80	3.987	38.19%	0.20	0.2499	20.8%
3	0.50	4.148	35.69%	0.50	0.2476	21.61%
4	0.20	5878	8.87%	0.80	0.2479	21.52%

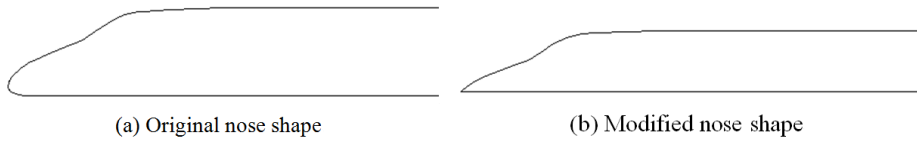


Figure 12: Nose shape of CRH2

#### 4 Conclusion

A new design technique for the nose shape of highspeed train under multi-line cases was proposed. This technique combining metamodel and optimization techniques, can balance the relations among different design objectives corresponding to different line cases. The method used here can easily be applied for a general three-dimensional nose shape design. Many further researches still need to be conducted in the future.

#### 5 Acknowledgements

The support from The National Key Technology R&D Program of China (2009 BAG 12A07), National High Technology Research and Development Program 863 (0912JJ0104-DL00-H-HZ-001-20100105) are acknowledged. The first author is also grateful the supports from China Scholarship Council (CSC) and Department of Applied Mathematics, Illinois Institute of Technology.

#### References

- Raghunathana, R. S.; Kimb, H. D. T.; Setoguchi, T.**(2002) :Setoguchic. Aerodynamics of high-speed railway train. *Progress in Aerospace Sciences*, vol.38, pp.469–514.
- Zhang, J.** (2005):Further research on optimum nose shape of high speed train. *Electric Locomotives & Mass Transit Vehicles*, vol.2, pp.5-8.
- Ogawa, T.; Fujii, K.** (1995):Effect of train shape on a compression wave generated by a train moving into a tunnel. *Proceedings of Korean Society of computational fluids engineering*.
- Ogawa, T.; Fujii, K.** (1996–1997): Theoretical algorithm to design a train shape for alleviating the booming noise at a tunnel exit. *J Jpn Soc Mech Eng* , vol.599, pp.2679–2686.
- Iida, M.; Matsumura, T.; Nakatani, K.; Fukuda, T.; Maeda, T.**(1997): Effective Nose Shape for Reducing Tunnel Sonic Boom. *QR of RTRI*, vol.38, pp. 206-211.

- Kwon, H. B.; Jang, K. H.; Kim, Y. S.; Lee, K. J.; Lee, D. H.** (2001): Nose shape optimization of high-speed train for minimization of tunnel sonic boom. *JSME IntJ Ser C*, vol.3, pp.890–899.
- Kwon, H. B.; Kim, Y. S.; Lee, D.H.; Kim, M.S.** (2001a): Nose shape optimization of the high-speed train to reduce the aerodynamic drag and micro-pressure wave. *Proceedings of the Korean Society of mechanical engineers*.
- Kwon, H. B.; Kim, T. Y.; Lee, D.H.; Kim, M. S.** (2001b): Numerical simulation of unsteady compressible flows induced by a high-speed train passing through a tunnel. *Proc Inst Mech Eng FJ Rail Rapid Transit*, vol.2, pp.111–124.
- Lee, J.; Kim, J.** (2008): Approximate optimization of high-speed train nose shape for reducing micro pressure wave. *Struct Multidisc Optim*, vol.1, pp.79–87.
- Ku, Y. C.; Rho, J.; Hyun.; Yun, S.H; Kwak, M. Ho.; Kim, K. H.; Kwon, H.B.; Lee, D. H.** Optimal cross-sectional area distribution of a high-speed train nose to minimize the tunnel micro-pressure wave. *Struct Multidisc Optim*, in press..
- Ku, Y. C.; Kwak, M.Ho.; Park, H.II.; Lee, D.H.**(2001): Multi-Objective Aerodynamic Shape Optimization of High-Speed Train Nose shape Using Vehicle Modeling function. 48th AIAA Aerospace Sciences Meeting Including the New Horizons Forum and Aerospace Exposition, pp.1501-1510
- Sun, Z. X.; Song, J. J.; An, Y. R.**(2010): Optimization of the head shape of the CRH3 high speed train. *Sci China Tech Sci*, vol.53, pp.3356-3364.
- Vytla, V. V.; S. K.**(2011): Multidisciplinary Optimization Framework for High Speed Train using Robust Hybrid GA-PSO Algorithm.thesis, Wright State University.
- Vytla, V. V.; Huangy, P. G.; Penmetsa, R. C.**(2010): Multi-Objective Aerodynamic Shape Optimization of High Speed Train Nose Using Adaptive Surrogate Model . *Proceeding of 28th AIAA Applied Aerodynamics Conference*, pp.4383-4395.
- Simpson, T. W.**(2001): Sampling Strategies for Computer Experiments. *Intl. J. of Reliability and Applications*, vol.2, pp.209-240.
- Joseph, A. S.**(2001): AERODYNAMICS OF HIGH-SPEED TRAINS. vol.38, pp.371–414.
- Bellenoue, M.; Morinie're, V.; Kageyama, T.**(2002): EXPERIMENTAL 3-D SIMULATION OF THE COMPRESSION WAVE, DUE TO TRAIN-TUNNEL ENTRY. *Journal of Fluids and Structures*, vol.5, pp.581–595.
- Siniša, K.**(2007): Aerodynamic optimization of vehicles using computational fluid dynamics and response surface methodology [J]. XXI Intl. JUMV Automotive Conference Science & Motor Vehicles.

**Sun, G. Y.; Li, G. Y.; Zhou, S. W.; Li, H. Z.; Hou, S. J.; Li, Q.**(2011): Crashworthiness design of vehicle by using multiobjective robust optimization. *Structural and Multidisciplinary Optimization*, vol.1, pp.99-110.

**Sun, G. Y.; Li, G. Y.; Zhou, S. W.; Xu, W.; Li, Q.**(2011): Multifidelity Optimization for Sheet Metal Forming Process. *Structural and Multidisciplinary Optimization*, vol.1, pp.111-124.

**Sun, G. Y.; Li, G. Y.; Gong, Z. H.; Cui, X. Y.; Li, Q.**(2010): Multiobjective robust optimization method for drawbead design in sheet metal forming. *Materials and Design*, vol.132, pp.1917-1929.

**Simpson, T. W.**(2001): Kriging models for global approximation in simulation-based multidisciplinary design optimization. *AIAA J*, vol.39, pp.2233–2241.

